J. Fluid Mech. (1982), *vol.* 120, *pp.* 463–473
Printed in Great Britain

The separation vortex in the Weis-Fogh circulation-generation mechanism

By R. H. EDWARDS AND H. K. CHENG
Department of Aerospace Engineering, University of Southern California, Los Angeles

(Received 8 September 1981 and in revised form 22 January 1982)

The influence of leading-edge separation vortices on the Weis-Fogh (1973) lift-generation mechanism for insect hovering is investigated. The analysis employs a vortex-shedding model (Edwards 1954; Cheng 1954) and represents an extension of Lighthill's (1973, 1975) analysis of an inviscid model without separated vortices. Results of the study compare reasonably well with observations on a laboratory model at high Reynolds number (Maxworthy 1979), confirming that vortex separation significantly enhances the initial circulation on each of the wings. Unlike the un-separated-model solution, this circulation was found to depend on the history of the wing motion and to increase with a large opening angle.

1. Introduction

Weis-Fogh (1973, 1975) described a model of insect flight which suggested a new mechanism for generating circulation. This technique requires the successive operations of the opening of a V-shaped wing segment and the subsequent separation of the two segments. Weis-Fogh's idea consists of producing equal and opposite circulations around the two segments without violating Kelvin's Theorem (and without shedding vortices), and subsequent generation of a lift from this circulation when the wings are parted.

The two dimensional definition of the Weis-Fogh mechanism is given in detail in Lighthill (1973), and it is shown schematically in figure 1, where AB and CD represent the chords of the wing pair. During the opening phase, the wings are pivoted about the point A, while during the spreading phase, the wings separate and move apart. We shall be concerned with the opening phase, and shall consider motion which starts from the 'clap' position which corresponds to $\alpha(0) = 0$, where $\alpha(t)$ is half of the opening angle as defined in figure 1. It must be pointed out that in addition to the original application to the study on the hovering of the tiny parasitic wasp *Encarsia* (Weis-Fogh 1973), recorded data on the widespread use of the clap–fling mechanism by the larger as well as the smaller insects are abundant. In particular, the hind-wing pair of *Locusta migratoria* is observed to undergo such a process even in forward, climbing flight, which is apparently also responsible for the noise production (Cooper & Baker 1977).

Lighthill (1973, 1975) presented a two-dimensional inviscid analysis of the opening phase, and also an examination of the modification of that analysis due to a leading-edge separation bubble. The latter appeared to give a rather weak effect of the leading-edge separation on the induced circulation. Subsequent experiments by Maxworthy (1979; also 1981), however, show a substantial effect of the leading-edge separation.

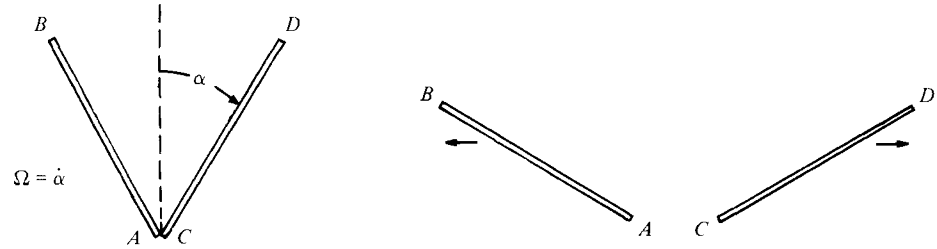

FIGURE 1. Illustration of the two phases in the Weis-Fogh mechanism.

The present work applies to this problem the model of a concentrated growing vortex pair, with feeder sheets, introduced and used rather successfully more than two decades ago by Edwards (1954) for slender delta wing problems, through an unsteady analogy. The model was extended to more general cases by Cheng (1954), where reasonable agreement of the nonlinear lift predicted by this model with the experiment of Winter (1936) is shown for rectangular wings with aspect ratio down to 1/30. In the present application, the vortex strength and vortex-centre location, obtained analytically for small time and numerically for large time, also agree rather well with the corresponding sequential photographs and the estimate of the vortex strength, made by Maxworthy (1979) for his mechanical model.

Shed vortices from a salient edge and their roll-up have been studied quite successfully by Chorin & Bernard (1973), Moore (1974), Sarpkaya (1975), Clements & Maull (1975), Fink & Soh (1978), Evans & Bloor (1977), Katz & Weihs (1978), and others, employing vortex-discretization methods. These treatments should yield good approximations to the problem at hand, although strictly speaking, none mentioned above may claim to approach the (inviscid) rolled-up sheet solution without empiricism. While the single-vortex model adopted here would be inadequate if the shed vorticity in the real flow changed sign, or if the sheet did not roll up, its adequacy appears to be well supported by laboratory observations for the present study; the relative simplicity enjoyed by the model renders much of its analytical properties tractable, as shown below. The model considered here may provide an alternative method for determining the strength and the location for the 'nascent vortices' essential to most existing vortex-discretization schemes. More recently, Guiraud & Zeytounian (1980) have developed an asymptotic theory for the spirally rolled-up vortex sheet and propose an analytical algorithm for computing the inviscid core. The present model corresponds to the outer solution in Guiraud & Zeytounian's theory. Their comparison remains to be studied.

In passing, we note that significant effects of vortex separation from leading edges of swept or delta wings are well known (Edwards 1954; Cheng 1954; Rott 1956), but they are not of first-order importance as long as these vortices lie close to the leading edges. In the analysis to follow, wherein the vortices are allowed to drift far away from the edges and to grow continuously, their circulations will be seen to be comparable to, or even greater than, the corresponding values of the unseparated potential model.

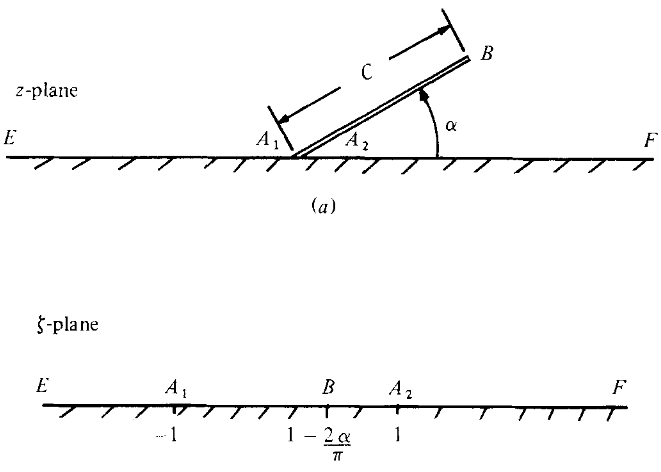

FIGURE 2. Mapping boundaries from z-plane to ζ-plane.

2. Analysis

2.1. *Lighthill's solution: closed-form expressions*

Following Lighthill (1973), we transform the problem from the physical z-plane to the ζ-plane with

$$\frac{d\zeta}{dz} = k\left(\frac{\zeta-1}{\zeta+1}\right)^{\alpha/\pi}\frac{\zeta-a}{\zeta+a}, \quad a = 1-\frac{2\alpha}{\pi}, \tag{1}$$

where k is a constant determined by the half-opening angle α and the chord length c (cf. figure 2). The complex potential $W_1 = \phi_1 + i\psi_1$ satisfying the instantaneous impermeable boundary condition on the wing AB in figure 2 and bounded everywhere is

$$W_1 = \Omega k^2(2\pi)^{-1}\int_{-1}^{1}(1+t)^{2-2\alpha/\pi}(1-t)^{2\alpha/\pi}(\zeta-t)^{-1}\,dt, \tag{2}$$

where $\Omega = \dot{\alpha}(t)$ is the instantaneous angular velocity of the wing. From this the potential jump across the wing at A can be determined as

$$\Gamma = \Omega c^2 g(\alpha). \tag{3}$$

Lighthill (1973) gave a numerical representation of $g(\alpha)$; an explicit value may, however, be found, and is given below. The relations between the z and ζ as well as the relation between W_1 and ζ are written in closed form as

$$z = k(1+\zeta)^{1-\alpha/\pi}(\zeta-1)^{\alpha/\pi}, \quad k = \tfrac{1}{2}c\left(1-\frac{\alpha}{\pi}\right)^{\alpha/\pi-1}\left(\frac{\alpha}{\pi}\right)^{-\alpha/\pi}, \tag{4}$$

$$W_1 = \frac{\Omega k^2}{2\sin 2\alpha}\left\{-(\zeta+1)^{2-2\alpha/\pi}(\zeta-1)^{2\alpha/\pi}+\zeta^2+\zeta\left(2-\frac{4\alpha}{\pi}\right)+\text{const}\right\}. \tag{5}$$

From (5), one finds

$$g(\alpha) = \left(1-2\frac{\alpha}{\pi}\right)\Big/2\,(\sin 2\alpha)\left(\frac{\alpha}{\pi}\right)^{2\alpha/\pi}\left(1-\frac{\alpha}{\pi}\right)^{2-2\alpha/\pi}. \tag{6}$$

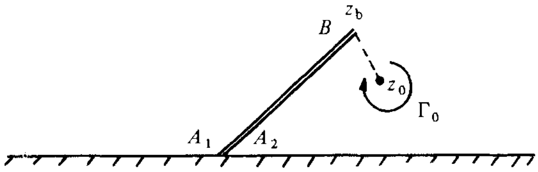

FIGURE 3. Illustration of the shed-vortex strength and location in the z-plane. Note the left-hand side of the sketch corresponds to the flow region on the lower side of the wing.

We note that Γ is a function only of the instantaneous value of Ω and α; thus it is independent of the history of the motion. The history, however, will be manifest through vortex shedding in the present model.

2.2. *The vortex-shedding model*

In our analysis, we adopt a model in which the total vorticity shed is concentrated in the single vortex at $z = z_0$ whose circulation Γ_0 is allowed to increase with time (cf. figure 3). This requires feeding of vorticity, and results in a non-vanishing pressure across a diaphragm (cut-line) of the unsteady potential. The resulting complex potential in the ζ-plane may then be represented by

$$W = W_1 + \frac{i\Gamma}{2\pi}\ln\frac{\zeta-\zeta_0}{\zeta-\bar{\zeta}_0}. \tag{7}$$

In order to satisfy momentum conservation in the crudest approximation, the total of forces on the vortex and the diaphragm must be zero. If the branch cut connects z_0 (vortex position) with z_b (wing-tip position), the complex force on the diaphragm is given by

$$F_1 = -\rho\dot{\Gamma}_0 i(z_0 - z_b), \tag{8}$$

where $\dot{\Gamma}_0$ is the strength of the shed vortex.

Similarly, the force on the vortex is given by

$$F_2 = \rho\Gamma_0 V^* i, \tag{9}$$

where V^* is the velocity of the local flow relative to the vortex, and is defined by

$$V^* = \lim_{z\to z_0}\overline{\left[\frac{dW}{dz} - \frac{i\Gamma_0}{2\pi(z-z_0)}\right]} - \dot{z}_0; \tag{10}$$

and the condition of a zero net force becomes

$$\Gamma_0^{-1}\frac{d}{dt}[\Gamma_0(z_0-z_b)] = -\dot{z}_b + \lim_{z\to z_0}\overline{\left[\frac{dW}{dz} - \frac{i\Gamma_0}{2\pi(z-z_0)}\right]}, \tag{11}$$

$$\frac{dW}{dz} = \frac{dW_1}{dz} + \frac{i\Gamma}{2\pi}\left(\frac{1}{\zeta-\zeta_0} - \frac{1}{\zeta-\bar{\zeta}_0}\right)\frac{d\zeta}{dz}, \tag{12}$$

where

$$\frac{d\zeta}{dz} = \left(\frac{d\zeta}{dz}\right)_{z_0} - \frac{z''}{z'^2}(\zeta-\zeta_0) + O[(\zeta-\zeta_0)^2], \tag{13}$$

$$\frac{i\Gamma_0}{2\pi(z-z_0)} = \frac{i\Gamma_0}{2\pi}\left[(\zeta-\zeta_0)^{-1}\left(\frac{d\zeta}{dz}\right)_{z_0} - \tfrac{1}{2}((z')^{-2}z')_{z_0}\right] + O[(\zeta-\zeta_0)]. \tag{14}$$

The primes denote derivatives with respect to ζ. Hence the terms that appear in brackets in (11) can be written as

$$\lim_{z\to z_0}\left[\frac{dW}{dz}-\frac{i\Gamma_0}{2\pi(z-z_0)}\right]=\left[\frac{dW}{dz}-\frac{i\Gamma_0}{2\pi}(\zeta-\bar{\zeta}_0)^{-1}\frac{d\zeta}{dz}-\frac{i\Gamma_0}{4\pi}(z')^{-2}z''\right]_{z_0}, \tag{15}$$

where
$$\frac{dW_1}{dz}=\frac{\Omega k^2}{\sin 2\alpha}\left\{(\zeta-1+2\alpha)\left[1-\left(\frac{\zeta+1}{\zeta-1}\right)^{1-2\alpha}\right]+2\left(1-2\frac{\alpha}{\pi}\right)\right\}\frac{d\zeta}{dz}, \tag{16}$$

and z' and z'' may be determined from (1).

Since the shedding of vorticity should result in the elimination of the infinite velocity at the edge, we impose a Kutta condition at the edge with the requirement

$$\frac{dW}{d\zeta}=0 \quad \text{at} \quad \zeta=a. \tag{17}$$

For this problem the Kutta condition takes the form

$$2k^2\Omega\,\frac{1-2\alpha/\pi}{\sin 2\alpha}=-\frac{i\Gamma_0}{2\pi}\,\frac{\zeta_0-\bar{\zeta}_0}{(1-2\alpha/\pi-\zeta_0)(1-2\alpha/\pi-\bar{\zeta}_0)}. \tag{18}$$

The governing equation for the motion of the vortex then becomes

$$\Gamma_0^{-1}\frac{d}{dt}[(z_0-z_{\mathrm{b}})\Gamma_0]=-i\Omega z_{\mathrm{b}}+\frac{i\Gamma_0}{4\pi}\,\overline{\frac{z''}{(z')^2}}+\overline{\frac{dW_1}{dz}}-\frac{i\Gamma_0}{2\pi}(\zeta_0-\bar{\zeta}_0)^{-1}\left(\overline{\frac{d\zeta}{dz}}\right)_{z_0}. \tag{19}$$

Equation (19) with (1), (4), (5) and (18) would yield definitions of z_0 and Γ_0 as functions of time provided that the history of the wing movement $z_{\mathrm{b}}(t)$ is given, and suitable initial values of z_0 are prescribed.

The shed vorticity corresponding to various forms of $\alpha(t)$ could be investigated. For example, if initially $\alpha(t) \neq 0$, $\Omega(t) \neq 0$, and the vortex is required to start from the leading edge, then

$$\Gamma_0/\Omega(0)c^2 \propto t^{\frac{1}{3}}, \quad (z_0-z_{\mathrm{b}})/ce^{i(\alpha_0-\frac{1}{2}\pi)} \propto t^{\frac{2}{3}}. \tag{20}$$

These results are identifiable with those of Cheng (1954) and Rott (1956).

2.3. *Behaviour when $\alpha \ll 1$*

The early stage of the flow development in the case which starts with the wing in the fully clapped position ($\alpha(0) = 0$) is of interest in the present study. We shall consider the case where the angular acceleration $\dot{\Omega}$ is initially finite, which was also the case studied in Maxworthy's experiments. For convenience, we define $\epsilon \equiv \alpha/\pi$, and shall be concerned first with the range of small ϵ.

We note that as ϵ approaches zero, ζ_0-1 and ζ_0-a both go to zero, since the vorticity is assumed to start from the leading edge. If $\zeta_0-1 \sim b\epsilon^n$ and if Γ_0 is non-decreasing, it can be shown that n must be greater than $\frac{1}{2}$; that $\Gamma_0^{-1}d[(z_0-z_{\mathrm{b}})\Gamma_0]/dt$ is of the order of $\epsilon^{n-\frac{1}{2}}$ if $n<1$, and of the order of $\epsilon^{\frac{1}{2}}\log\epsilon$ if $n>1$. Hence, the left-hand side of (19) is zero or finite as ϵ approaches zero. Several of the terms on the right-hand side of (19) can be seen to be singular as ϵ approaches zero, and a cancellation is necessary in order to balance the left-hand side.

The right-hand side of (19) has the representation

$$-i\Omega z_0+i\Gamma_0\left(\overline{\frac{d\zeta}{dz}}\right)_{z_0}\left\{-\frac{\epsilon}{\bar{\zeta}_0+1}+\frac{\epsilon-1}{\bar{\zeta}_0-1}+\frac{1}{\bar{\zeta}_0-1+2\epsilon}-\frac{2}{\zeta_0-\bar{\zeta}_0}\right.$$
$$\left.+\frac{1}{2\epsilon}\frac{\zeta_0-\bar{\zeta}_0}{(\zeta_0-1+2\epsilon)(\bar{\zeta}_0-1+2\epsilon)}\left[(\bar{\zeta}_0-1+2\epsilon)\left(1-\left(\frac{\bar{\zeta}_0+1}{\bar{\zeta}_0-1}\right)\right)^{1-2\epsilon}+2(1-2\epsilon)\right]\right\}, \quad (21)$$

where

$$\left(\overline{\frac{d\zeta}{dz}}\right)_{z_0}=k^{-1}\left(\frac{\bar{\zeta}_0+1}{\bar{\zeta}_0-1}\right)^{\epsilon}\frac{\bar{\zeta}_0-1}{\bar{\zeta}_0-1+2\epsilon}, \quad (22)$$

$$\frac{i\Gamma_0}{2\pi}=\frac{2k^2\Omega(1-2\epsilon)}{\sin 2\pi\epsilon}\frac{(\zeta_0-1+2\epsilon)(\bar{\zeta}_0-1+2\epsilon)}{\zeta_0-\bar{\zeta}_0}. \quad (23)$$

The only expansion that has been found to provide the proper balancing of the left- and right-hand sides of (19) consistent with $\epsilon \ll 1$ is of the type

$$\left.\begin{aligned}\mathscr{R}(\zeta_0-1) &\sim -3\epsilon^2\\ \mathscr{I}(\zeta_0-1) &\sim \sqrt{2}\epsilon^{\frac{3}{2}}.\end{aligned}\right\} \quad (24)$$

The corresponding position of the vortex is given by

$$z_0 \sim c(1+\epsilon)\left(\tfrac{1}{2}(1-\epsilon)\right)^{\epsilon}\left(1+\tfrac{1}{2}\epsilon\ln 2\epsilon+i\epsilon\arctan\left(-\tfrac{1}{3}\sqrt{2}\epsilon^{-\frac{1}{2}}\right)\right), \quad (25)$$

subject to error at most $O(\epsilon^{\frac{3}{2}}\ln\epsilon)$. It is understood that the angle defined by the inverse tangent is in the second quadrant. For $\epsilon \ll 1$, this angle is approximately $\frac{1}{2}\pi$, so that the term $i\epsilon\arctan(-\frac{1}{3}\sqrt{2}\epsilon^{-\frac{1}{2}})$ tends to $\frac{1}{2}i\epsilon\pi = \frac{1}{2}i\alpha$. Since $z_b = ce^{i\alpha}$, and, for small α, $z_0 = ce^{-\frac{1}{2}i\alpha}$ the vortex is accordingly midway between the initial and instantaneous position of the wing tip, subject to a relative error $O(\epsilon^{\frac{1}{2}}\ln\epsilon)$.

Note that the strength of the shed vortex starts with a finite value for the case considered. In fact, if $\Omega \sim \beta t$, then

$$\Gamma_0 \sim c^2(\pi\beta)^{\frac{1}{2}} \neq 0, \quad (26)$$

which signifies a very rapid build-up of the vortex strength during the initial phase (cf. §4).

Consider next the effect of the shed vorticity Γ_0 on the circulation about one segment of the wing. The additional circulation due to the shed vortex can be evaluated simply in the ζ-plane from the change in potential between points A_1 and A_2 due to Γ_0, by

$$\Delta\phi=\frac{\Gamma_0}{\pi}\gamma=\frac{\Gamma_0}{\pi}\left(\arctan\frac{m}{1+l}+\arctan\frac{m}{1-l}\right)\sim\frac{\Gamma_0}{\pi}\left(\tfrac{1}{2}\pi-\frac{3}{\sqrt{2}}\epsilon^{\frac{1}{2}}\right), \quad (27)$$

where l and m are respectively the real and imaginary parts of ζ_0 and γ is the angle in the ζ-plane shown in figure 4. Thus, for small angle, $\Delta\phi \sim \frac{1}{2}\Gamma_0$.

The above result differs from the conclusion of Lighthill (1975) that the effect of shed vorticity on the induced circulation would be small. This difference is in the placement of the shed vortex, which results in the difference in the value of γ. Lighthill assumed that both $m/(1-l)$ and $m/(1+l)$ would be small compared with one, whereas, from the present analysis, $m/(1-l)$ is found to be large for small values of ϵ, and γ is consequently close to $\frac{1}{2}\pi$. With this model, the vortex does originate at the leading edge, but it moves away from the wing in such a way that ζ_0-1 is initially imaginary. The result of this behaviour is that, for small opening angles, the circulation about each half-wing is increased by half of the strength of each shed vortex.

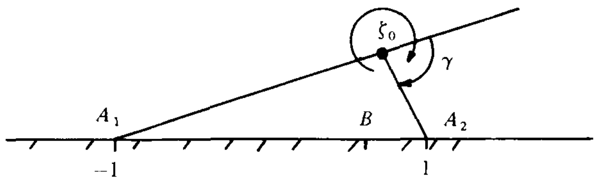

FIGURE 4. Illustration of the angle γ in the ζ-plane.

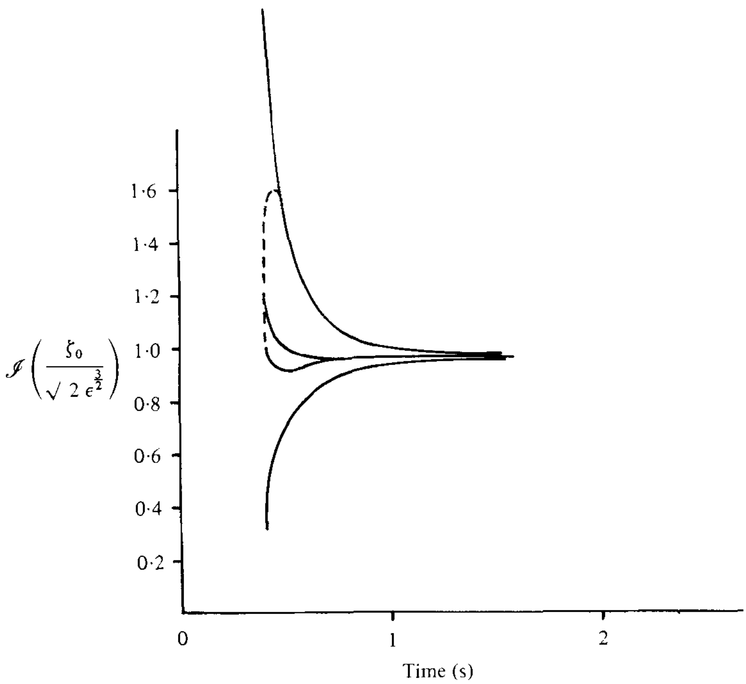

FIGURE 5. Test of stability of the solution obtained for small ϵ with respect to differences in initial data.

2.4. *Integration to large t*

Equation (19), with the explicit form for its right-hand side given by (21), together with the Kutta condition (23), can be integrated numerically forward in time t from a given initial value of ζ_0 at a chosen $t = t_0$. For the present purpose, we choose a small enough t_0 so that the initial data can be described with sufficient accuracy by the asymptotic solution for small t in §2.3. The type of small-time solution will depend on the early behaviour of $\ddot{\alpha}$. Specific numerical integrations have been performed for the history of $\alpha(t)$ corresponding closely to the laboratory mechanical model studied by Maxworthy (1979), in which the $\alpha(t)$ history has a non-zero initial angular acceleration (cf. §3 and figure 6).

The small-time solutions corresponding to (24) are input as initial data. Small differences in the initial data are purposely introduced in some trial runs to confirm stability. In figure 5, $\mathscr{I}(\zeta_0 - 1)\,(2\epsilon^3)^{-\frac{1}{2}}$ is plotted against time for various initial conditions. The results are seen to converge to a common value by $t = 1{\cdot}5$. In these curves, initial real parts of $\zeta_0 - 1$ are all close to unity, differing from unity by amounts comparable to 10^{-3}.

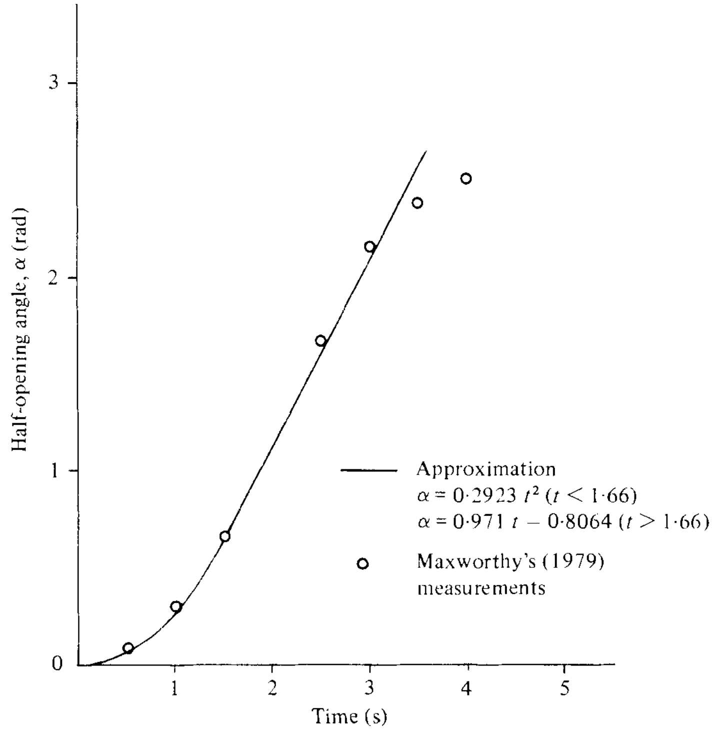

FIGURE 6. Comparison of the approximate representation of $\alpha(t)$ with Maxworthy's record of the opening angle.

3. Comparison with experiment

Maxworthy (1979) reported vortex measurements at two values of Reynolds number, one at $Re = 13\,000$ and the other at $Re = 32$. Since the foregoing analysis is applicable primarily to higher-Reynolds-number phenomena, we will compare the results of this study with his case where $Re = 13\,000$. In this connection, one may recall the widespread use of the clap–fling process by the larger insects noted earlier.

The time history of the opening angle is shown in figure 6. For calculational purposes, we approximate this history over the major portion of the time by

$$\begin{aligned}\Omega &= 0{\cdot}5847t\,\text{rad/s} \quad (t \leqslant 1{\cdot}66\text{ s})\\ &= 0{\cdot}971\text{ rad/s} \quad (t > 1{\cdot}66\text{ s}).\end{aligned}$$

Equation (19) was integrated from $t = 0{\cdot}4$ s, corresponding to $\epsilon = 0{\cdot}0149$, with the small-ϵ approximation of (24) used at that point. Comparisons of the values of Γ with Maxworthy's measured values and with Lighthill's value with no separation are shown in figure 7. Here, since Ω is a function of the opening angle, the theoretical values of Lighthill have been multiplied by Ω, and the curves display the values of Γ/c^2 rather than the dimensionless $\Gamma/c^2\Omega$. In Maxworthy (1979) the results had been plotted as $\Gamma/c^2\bar{\Omega}$, where $\bar{\Omega}$ was an average value of Ω taken to be approximately 1·15 rad/s, so that the experimental Γ/c^2 plotted here is 1·15 times his $\Gamma/c^2\bar{\Omega}$. As can be seen, the measured values of Γ are well above the inviscid, non-separated values, while our model results are within the error estimates of Maxworthy's measurements up to $\alpha = 100°$.

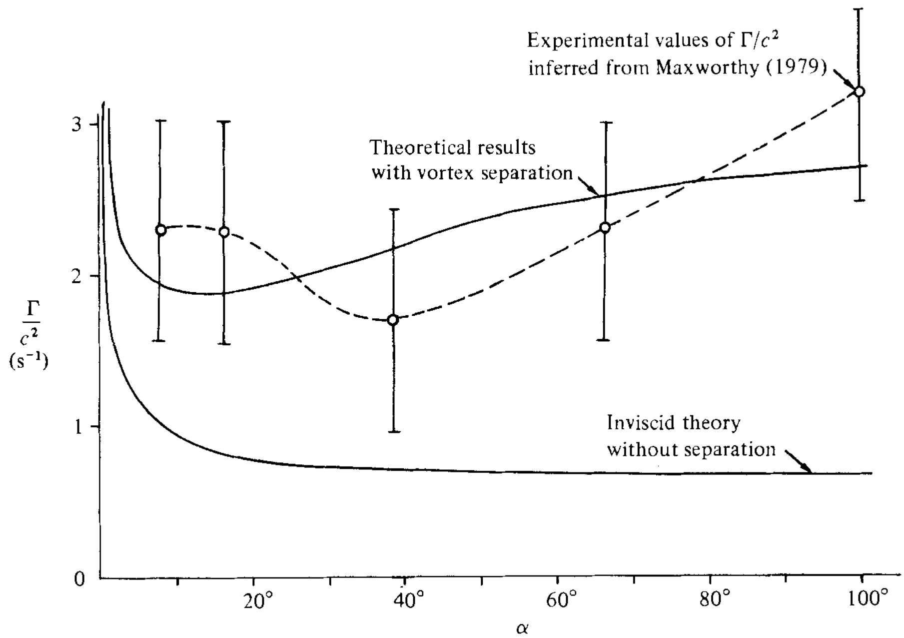

FIGURE 7. Comparison of the potential jump at A predicted by the theory with data inferred from Maxworthy's laboratory data and with results from Lighthill's analysis.

We note that the value of γ of the theory (cf. (27)) was found to stay close to $\frac{1}{2}\pi$ throughout the process; accordingly, the change in circulation over each half-wing is closely approximated by $\frac{1}{2}\Gamma_0(t)$.

Interestingly, both the present theory and Maxworthy's (1979) laboratory observations indicate that, unlike the results for the unseparated-flow model, the circulation Γ in question does not decrease with increasing opening angle, even at $\alpha = 90°$ and beyond. Thus it may seem advantageous for a hovering insect to commence the spreading phase at an opening angle as large as 90° in order to gain a high initial circulation, although it may decrease subsequently as a result of vortex shedding.

A peculiar feature of the present solution is the finite initial vortex strength Γ_0, proportional to the initial angular acceleration $\ddot{\alpha}(0)$ or $\dot{\Omega}(0)$, which may be interpreted as indicating an extremely high initial growth rate, as noted in §2.3. This notion appears to be consistent with the relatively high values of Γ inferred from Maxworthy's laboratory data (open circles) for the smaller values of α in figure 7. At an extremely small opening angle, an inviscid model is expected to break down, and the initial flow data for the subsequent inviscid calculation should be provided for by a viscous-flow solution. Recirculatory flow patterns in the interior of a corner are possible solutions to the Stokes equations (Moffatt 1964), therefore admissibility of a $\Gamma_0(0) \neq 0$ to the present inviscid model should not be too surprising. We also recall in this connection that stability of our small-α solution has been tested and confirmed in §2.4.

Figure 8 shows the predicted sequential locations of the vortex centre (indicated by white crosses), superimposed on the corresponding photo records furnished by Professor Maxworthy. Considering the rather idealized representation of the single-vortex model, the agreement must be considered to be encouraging.

One may recall from §2.3 (25), that at small ϵ, the vortex centre stays close to the

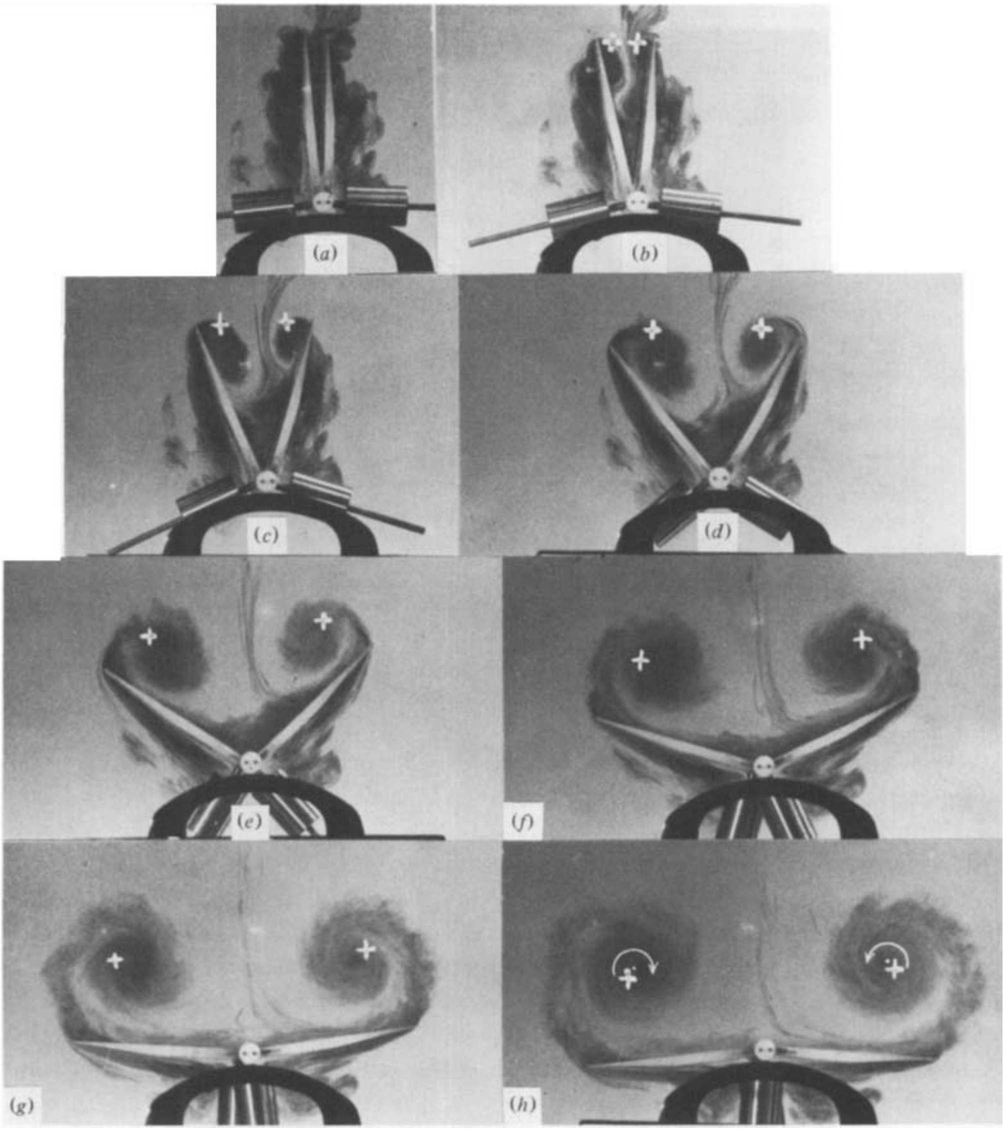

FIGURE 8. The vortex-centre location (white crosses) of the shedding-vortex solution marked against Maxworthy's (1979) photo record.

bisector of the half-opening angle; this is observed from the photo records to hold up to $\alpha = 45°$. For larger angles ($\alpha > 45°$), the vortex position was found to shift along a line which makes an angle of about $\frac{2}{3}\alpha$ with the centre line.

4. Concluding remarks

Lighthill's (1973, 1975) analysis of the Weis-Fogh circulation-generation mechanism is extended to allow for the treatment of vortex shedding from the salient edges. The basic vortex-shedding model employed is that introduced earlier by Edwards (1954), extended and studied by Cheng (1954) and Rott (1956). Applied to the present problem, the vortex shedding is shown to have an important influence on the flow field. Consequential to the separation, the circulation on each member of the wing pair is significantly augmented over most of the range of the opening angle, thus greatly enhancing the Joukowski lift as perceived originally by Weis-Fogh (1973). The growth rate of the vortex strength as well as the vortex-centre movement predicted by the present analysis are found to be consistent with laboratory data in the higher-Reynolds-number case reported by Maxworthy (1979), within the margin of experimental errors.

Whereas the key to the success of Weis-Fogh's (1973) clap–fling mechanism is the *circulation* Γ achieved by each wing at the end of the opening phase, its significance lies entirely on the influence of this Γ on the subsequent *lift development* during the spreading phase, which is not determined by the initial Joukowski lift $\rho U \Gamma$ alone (where U is the instantaneous relative velocity). If the vortex produced by opening is not consistent with that required to give the quasi-steady lift during the fling process, then either some vorticity will be shed or more will be produced by leading-edge separation. With the presence of a wing on the other side and the shed vorticities from both, it is not altogether clear, without further analysis, whether or not this model insect wing may indeed serve as a lift generator far superior to those in classical aerodynamics (Wagner 1925). Of no less importance is the evaluation of the force experienced by, as well as moment and power required of, an insect during the open phase of this model. These answers will again depend on history of the motion in the presence of shed vortices, and can be calculated as an extension of the present analysis.

This study was supported by the U.S. National Science Foundation, Engineering Division, Contract Number CME-7926003. We would like to express our deep appreciation of the valuable comments and helpful suggestions given on this study by Professor Sir James Lighthill and Professor T. Maxworthy, who also furnished some of the original data and photo records of his previous work.

REFERENCES

Cheng, H. K. 1954 *J. Aero. Sci.* **21**, 212.

Chorin, A. J. & Bernard, P. S. 1973 *J. Comp. Phys.* **13**, 423.

Clements, R. R. & Maull, D. J. 1975 *Prog. Aero. Sci.* **16**, 129.

Cooper, R. J. & Baker, P. S. 1977 *Nature* **269**, 53.

Edwards, R. H. 1954 *J. Aero. Sci.* **21**, 13.

Evans, R. A. & Bloor, M. I. G. 1977 *J. Fluid Mech.* **82**, 115.

Fink, P. T. & Soh, W. K. 1978 *Proc. R. Soc.* A **362**, 195.

Guiraud, J. P. & Zeytounian, R. Kh. 1980 *J. Fluid Mech.* **101**, 393.

Katz, J. & Weihs, D. 1978 *J. Aircraft* **15**, 871.

Lighthill, M. J. 1973 *J. Fluid Mech.* **60**, 1.

Lighthill, M. J. 1975 *Mathematical Biofluiddynamics*. SIAM.

Maxworthy, T. 1979 *J. Fluid Mech.* **93**, 47.

Maxworthy, T. 1981 *Ann. Rev. Fluid Mech.* **13**, 329.

Moffatt, H. K. 1964 *J. Fluid Mech.* **18**, 1.

Moore, D. W. *J. Fluid Mech.* **63**, 225.

Rott, N. 1956 *J. Fluid Mech.* **1**, 111.

Sarpkaya, T. 1975 *J. Fluid Mech.* **68**, 109.

Wagner, H. 1925 *Z. angew Math. Mech.* **5**, 17.

Weis-Fogh, T. 1973 *J. Exp. Biol.* **59**, 169.

Weis-Fogh, T. 1975 In *Swimming and Flying in Nature* (ed. T. Y. T. Wu, C. J. Brokaw & C. Brennan) vol. II, p. 729. Plenum.

Winter, H. 1936 Strömungsvorgange an Platten und Profilerten Körpern bei Spannweiten, V.D.I.; English transl. *NACA TM* 798.